Stability of flexible thin-film metallization stimulation electrodes: analysis of explants after first-in-human study and improvement of in vivo performance

Paul Čvančara, Tim Boretius, Víctor López-Álvarez, Pawel Maciejasz, David Andreu, Stanisa Raspopovic, Francesco M. Petrini, Silvestro Micera, Giuseppe Granata, Eduardo Fernandez, et al.

Journal of Neural Engineering

PAPER

Stability of flexible thin-film metallization stimulation electrodes: analysis of explants after first-in-human study and improvement of *in vivo* performance

Paul Čvančara[1,16] ⓘ, Tim Boretius[2], Víctor M López-Álvarez[3], Pawel Maciejasz[4], David Andreu[4],
Stanisa Raspopovic[5], Francesco Petrini[5,6], Silvestro Micera[6,7], Giuseppe Granata[8], Eduardo Fernandez[9],
Paolo M Rossini[8,10], Ken Yoshida[11], Winnie Jensen[12], Jean-Louis Divoux[13], David Guiraud[4] ⓘ, Xavier Navarro[3]
and Thomas Stieglitz[1,14,15] ⓘ

[1] Laboratory for Biomedical Microtechnology, Department of Microsystems Engineering – IMTEK, Albert-Ludwig-University Freiburg, Freiburg, Germany
[2] neuroloop GmbH, Freiburg, Germany
[3] Department of Cell Biology, Physiology and Immunology and Institute of Neurosciences, Universitat Autònoma de Barcelona (UAB), and CIBERNED, Bellaterra, Spain
[4] Camin Team, INRIA, University of Montpellier, Montpellier, France
[5] Laboratory for Neuroengineering, Department of Health Sciences and Technology, Institute for Robotics and Intelligent Systems, ETH Zürich, Zürich, Switzerland
[6] Center for Neuroprosthetics and Institute of Bioengineering, School of Engineering, École Polytechnique Fédérale de Lausanne (EPFL), Lausanne, Switzerland
[7] The Biorobotics Institute, Scuola Superiore Sant'Anna, Pisa, Italy
[8] Institute of Neurology, Catholic University of the Sacred Heart, Roma, Italy
[9] Institute of Neurosurgery, Catholic University of the Sacred Heart, Roma, Italy
[10] Polyclinic A. Gemelli Foundation-IRCCS, Roma, Italy
[11] Biomedical Engineering Department, Indiana University-Purdue University, Indianapolis, Indiana, United States of America
[12] SMI, Dept. Health Science and Technology, Aalborg University, Aalborg, Denmark
[13] A!MD: Advice In Medical Devices, France
[14] BrainLinks-BrainTools, Albert-Ludwig-University Freiburg, Freiburg, Germany
[15] Bernstein Center Freiburg, Albert-Ludwig-University Freiburg, Freiburg, Germany
[16] Author to whom any correspondence should be addressed.

E-mail: paul.cvancara@imtek.uni-freiburg.de

Abstract

Objective. Micro-fabricated neural interfaces based on polyimide (PI) are achieving increasing importance in translational research. The ability to produce well-defined micro-structures with properties that include chemical inertness, mechanical flexibility and low water uptake are key advantages for these devices. *Approach.* This paper reports the development of the transverse intrafascicular multichannel electrode (TIME) used to deliver intraneural sensory feedback to an upper-limb amputee in combination with a sensorized hand prosthesis. A failure mode analysis on the explanted devices was performed after a first-in-human study limited to 30 d. *Main results.* About 90% of the stimulation contact sites of the TIMEs maintained electrical functionality and stability during the full implant period. However, optical analysis post-explantation revealed that 62.5% of the stimulation contacts showed signs of delamination at the metallization-PI interface. Such damage likely occurred due to handling during explantation and subsequent analysis, since a significant change in impedance was not observed *in vivo*. Nevertheless, whereas device integrity is mandatory for long-term functionality in chronic implantation, measures to increase the bonding strength of the metallization-PI interface deserve further investigation. We report here that silicon carbide (SiC) is an effective adhesion-promoting layer resisting heavy electrical stimulation conditions within a rodent animal trial. Optical analysis of the new electrodes revealed that the metallization remained unaltered after delivering over 14 million pulses *in vivo* without signs of delamination at the metallization-PI interface. *Significance.* Failure mode analysis guided implant

stability optimization. Reliable adhesion of thin-film metallization to substrate has been proven using SiC, improving the potential transfer of micro-fabricated neural electrodes for chronic clinical applications. (Document number of Ethical Committee: P/905/CE/2012; Date of approval: 2012–10-04)

1. Introduction

In recent years, micro-fabricated devices initially developed for use as high resolution tools in neuroscientific animal research have entered translational research in human clinical trials. To interface the nervous system electrically, various designs and approaches have been proposed [1]. Devices and techniques vary in their degree of invasiveness and selectivity [2], ranging from electrodes that lay superficially on or around the target tissue, for example electrocorticogram (ECoG) electrodes [3] or cuff electrodes [4, 5], to more invasive devices that penetrate the tissue, such as intracortical microelectrode arrays (MEA) or intraneural Utah slanted electrode arrays (USEA) [6, 7]. Electrode materials and coatings need to be selected according to the manufacturing technology [2, 8] and target application [9]. Among the possible polymers utilized for miniaturized nerve interfaces, polyimide (PI) comes along with certain benefits [10]. In comparison to silicone rubber, it is possible to achieve device thicknesses, about 10 times thinner, which help to reduce the insertion trauma for intraneural and intracortical applications. Further benefits are high chemical inertness and flexibility compared to silicon and metal wires and in case of the PI type utilized within this study, the water uptake is with 0.5% very low [10]. Moreover, fabrication using standard photolithographic processes is feasible. *In vitro* characterization indicated the possibility of using PI as substrate material for chronic application (>30 d) [11]. Even though plenty of studies on preclinical assessments in acute and chronic animal models as well as clinical intraoperative monitoring and first-in-human clinical trials have been published, there is a lack of device assessment and especially electrode stability evaluation post explantation. Therefore, our team decided to share data from a pilot study with one subject to report failure modes as well as actions and measures to increase stability of thin-film electrodes for neural stimulation. We hope to encourage others to share failure mode data with the scientific community in order to join forces on the way to miniaturized neural stimulation implants. Good scientific practice should not be limited to sound methods and data processing but also to publish functional failures to prevent spreading of hazards due to missing information.

Promising stability of polyimide recording arrays with thin-film metallization in non-human primates have been reported by Rubehn *et al* showing chronically stable recording of brain signals with a micro-fabricated 252-channel ECoG *in vivo* in Rhesus monkey [3]. Given the possibility of chronic recording stability, the next challenge emerged: Is chronically stable stimulation possible with micro-fabricated PI electrodes?

Electrical stimulation through thin-film structures presents several challenges not seen when the devices are used for recording. The stimulation contact site must be able to transmit electrical current at a sufficient level to activate the nerve fibers without eroding or damaging the contact or electrode structure. For micro-stimulation through contacts of sizes in the 10 s of μm, the safe current density limits become a challenge due to the small area of the contact [12]. For our application, i.e. multi-channel micro-stimulation of human peripheral nerves, the relatively large size of the nerve bundle further increases the challenge since guidance and spreading of the current into the larger nerve bundle requires larger currents as compared to those needed for smaller nerve bundles in small animal models. We converged to an intrafascicular approach in this particular application, since such a device places the electrode contacts within the nerve bundle, and thus achieves a more focal activation of nerve fibers while minimizing the current needed for activation. However, this approach requires multiple sites of stimulation within a given nerve fascicle or in several nerve fascicles to provide different types of sensations and cover the largest possible sensory field. Our group developed the transverse intrafascicular multichannel electrode (TIME) [13], to increase the spatial selectivity of peripheral nerve stimulation electrodes, compared to cuff and longitudinal intrafascicular electrodes (LIFEs) [14]. The TIME is implanted perpendicularly to the axis of the nerve fascicle, in order to address as many fascicles as possible and thus to increase the stimulation selectivity. To decrease the probability of nerve damage, polyimide was chosen as substrate material due to its mechanical properties and manufacturing technologies, that allowed for thin, shallow and flexible devices with adequate strength for handling during implantation and mechanical load during the implantation period. Through evaluation of devices has been performed during the design and development process [15]. The final documentation has been handed in to and approved by the respective legal authorities (Italy,

Denmark, Switzerland) before a first-in-human clinical trial has been performed. Electrical stimulation stability of the thin-film electrodes has been performed *in vitro*, first. Electrical Impedance Spectroscopy was used to monitor the transfer characteristics in general, whole cyclic voltammetry was used to identify the limits of the water window and measure the charge storage capacity (C_{CSC}) [15, 16]. Voltage transient measures during current-controlled stimulation determined the charge injection capacity to 60 nC. Stimulation with one billion pulses using constant charge of 60 nC per phase (200 μs * 300 μA) in phosphate buffered saline (PBS) solution revealed no significant change in the electrochemical properties [16, 17]. Neither scanning electron microscopy (SEM) nor atomic force microscopy (AFM) revealed any morphological changes nor mechanical disintegration [15].

Mechanical stability tests of the cables with respect to bending and stretching as well as to mechanical impact verified adequate stability of the chosen helical approach of multi-strand cables [15].

Acute and systemic cytotoxicity has been evaluated according to ISO standard 10993–5 and ISO 10993–12 with samples that underwent the whole micromachining process [15, 18].

Comprehensive preclinical evaluation of the TIME in small and large animal models [14, 19–21] has been performed on rodents as well as on acute and chronic pig models. Electrical stimulation performance was reliable in the sub-chronic study up to 30 d. Based on these positive and successful data, a first-in-human study was conducted with an implantation period of 30 d [22, 23], that has been chosen according to European medical device regulations. The aim was to stimulate the median and ulnar nerves in the stump of an arm amputee to evoke sensations at high spatial resolution, with the aim to reduce phantom limb pain and to deliver sensory feedback from a sensorized hand prosthesis governed via electromyographic voluntary commands from the stump residual muscles. The outcome of the clinical trial was very satisfying, showing the possibility of delivering near-natural sensory information to the patient by stimulation of the peripheral nerves during real-time decoding of grasping objects of different physical properties with the hand-prosthesis. It was possible for the patient to modulate the grasping forces of the hand-prosthesis and to recognize objects with different shape and compliance even when visual and auditory inputs were avoided [22]. Moreover, the amputee was able to discriminate with artificial fingertips the spatial coarseness [23] of a moving surface. All four TIME devices were explanted at the end of this clinical study.

We report in this work about the results of the investigations of the integrity of the thin-film TIMEs from the afore-mentioned first-in-human study, regarding the electrical properties and the mechanical integrity post explantation. Although the *in vivo* impedance measurements were excellent and patient responses to electrical stimulation via the TIMEs were stable up to the last day of implantation, we observed mechanical failure of the thin-film metallization after explantation, although none of the preceding *in vitro* and *in vivo* experiments indicated any of these kind of malfunctions. Consequently, we had to take measures to improve the mechanical stability of the thin-film metallization, in order to ensure good performance over much longer periods of *in vivo* implantation and reduce the risk of failure for any future applications. For this purpose, we introduced silicon carbide (SiC) as adhesion promoting layer between PI and platinum, according to our previous *in vitro* research [1, 24, 25]. The *in vivo* validation was performed in a small animal model (Sprague-Dawley rats). Optical analysis confirmed that the mechanical integrity of the thin-film electrodes was improved significantly using SiC as adhesion promoting layer.

Inside the scientific community of neural prosthetic devices only little is reported sincerely on failure mechanisms and the consequences [26–29]. We believe that it is an important contribution in translational research to share knowledge on the way to safe and reliable implants and reduce the risk of failure in any volunteering subject in research.

2. Materials and methods

The TIME implants consist of a PI-based thin-film electrode array, attached to a helically wound cable (MP35 N) via an interconnecting ceramic, that terminates in a commercially available connector. The human version is called TIME-3 H while the samples in the subsequent animal study for investigation on the efficacy of applied measures to improve thin-film adhesion were called TIME-RMI. The following paragraphs describe the design and the analysis of the human implant that has been analyzed after a 30 d first-in-human study as well as the improvement of the thin-film array and its validation in an animal model.

2.1. Analysis of TIME-3 H from sub-chronic first-in-human clinical trial

The focus of this work was the evaluation of the TIME-3 H implant of a sub-chronic first-in-human clinical trial which results and outcome have been described in detail previously [22]. The TIME-3 H have been tested comprehensively in preclinical studies for the envisioned 30 d implantation time of the human study with respect to foreign body reactions [18], scarring [19], acute selectivity [14] and chronic functionality [21] and stability [19]. Analysis of results were input parameters into a risk assessment according to ISO 14971 from which reasonably low risk level for the patient was concluded.

2.1.1. Design and cleanroom fabrication of the thin-film electrodes.

The version TIME-3 H (details in [17]), used in the first-in-human study sub-chronically (i.e. 30 d), contained 18 channels, of which 16 correspond to stimulation contact sites (only 14 connected, due to the limited number of channels in the connector) and two ground contacts. After folding, the electrode displayed seven connected stimulation contact sites on the left and seven on the right, named L1 to L7 and R1 to R7 respectively. The same applied for the two ground contacts, L GND and R GND. The stimulation contact sites had a circular shape with a diameter of 80 μm. The large ground sites exhibited a rectangular shape with an area of 1.00×0.25 mm^2 each. Platinum tracks and pads were sandwiched between polyimide as substrate and insulation layer. At the stimulation and ground contact sites, the platinum layer was coated by iridium, subsequently covered by a sputtered iridium oxide film (SIROF) (figure 1(a) top) and opened via reactive ion etching (RIE).

The general design and layout of the TIMEs used in human and in the subsequent rodent animal trial are identical, but the layer setup is varied (with and without silicon carbide; figure 1(a) bottom).

The thin-film electrode arrays of the TIME implants were fabricated using standard processing of microelectromechanical systems (MEMS) within a clean room environment. Both thin-film electrode versions (sub-chronic human clinical trial and small animal validation) used polyimide (U-Varnish S, UBE Industries, LTD., Tokyo, Japan) as substrate and insulation material. The thin-film electrodes for the TIME-3 H were fabricated according to previously published processes [13, 17]. Further process details can be found in the supplementary materials.

Following the last fabrication step, the thin-film electrodes were peeled off the silicon wafer with a pair of forceps (figure S2f (stacks.iop.org/JNE/17/046006/mmedia)) for assembly of the implants.

2.1.2. Implant assembly.

The TIME-3 H implants (hereafter called TIME) were assembled out of four sub-modules (for details see [17] and figure 1(b)). First, the thin-film part containing the stimulation contacts and the ground contacts to close the electrical circuit during stimulation. Second, a screen-printed interconnecting ceramic to mechanically and electrically connect the thin-film electrode to the third part, a 40 cm long cable. The fourth module was a commercially available connector (NCP-16-DD, Omnetics Connector Corporation, Minneapolis, USA).

2.1.3. Clinical study.

The patient was a 36-year-old male, suffering from a traumatic transradial amputation of the left arm ten years before implantation. The subject was implanted with TIME 1 and 2 in the median nerve (proximal and distal) and TIME 3 and 4 in the ulnar nerve (proximal and distal). The implantation surgery was conducted on 26th of January 2013 (figure 1(d)) at the Polyclinic A. Gemelli at the Catholic University, Rome, Italy after obtaining the ethical approval. The patient signed an informed consent form before the beginning of the study. For all experiments conducted in the study, the respective EU guidelines and regulations were considered.

At the end of the 30 days' limit of the clinical trial, the implants were removed according to the clinical protocol. The patient underwent a six months' follow-up after finishing the clinical trial and did not reveal any side-effects, neither objective nor subjective. After explantation the implants were stored in PBS for transport, rinsed in deionized water and dried with nitrogen. The implants were stored in dry atmosphere and light protected. Since the surgeon had to prioritize the integrity and function of the patient's nerves over the integrity of the TIMEs during the explantation procedure, the electrode arrays were mostly separated from cables and connectors and cut in 'bits and pieces', also to reduce the time of the surgical intervention.

2.1.4. Electrical characterization of the TIMEs in vivo (human).

Data during in vivo experiments were acquired by the STIM'nD stimulator (max. output current 5 mA at a maximum of 20 V) and associated software provided by INRIA (Montpellier, France). The electrochemical impedance of each stimulation contact site and the ground contacts of the four implanted TIMEs was estimated using an indirect method that is well established in clinical neural implants and gives an adequate estimation of the charge injection capacity and variations at the material-tissue interface [31, 32]. For this purpose, a very small controlled-current stimulus (balanced biphasic rectangular pulses of I = 40 μA and t = 300 μs per phase) was generated using each active contact site separately (cathodic phase first) and one ground contact site. A resistor of R = 1 kΩ was inserted in series with the TIME implant to monitor the current. While generating the stimulus, the voltage-drop between cathode and anode as well as the voltage-drop at the resistor were measured (insulated NI6218, National Instrument, Austin, Texas, USA) with an acquisition frequency of 100 kSs^{-1}. The magnitude of the impedance of each stimulation contact site versus each of the two ground contacts (left and right) as well as between the two ground contacts of each TIME was determined as the ratio of the voltage excursion at the end of the cathodic phase divided by the current amplitude of the stimulation pulse. Depending on the orientation of the ground electrode to the nerve after implantation (i.e. either facing the nerve side or facing
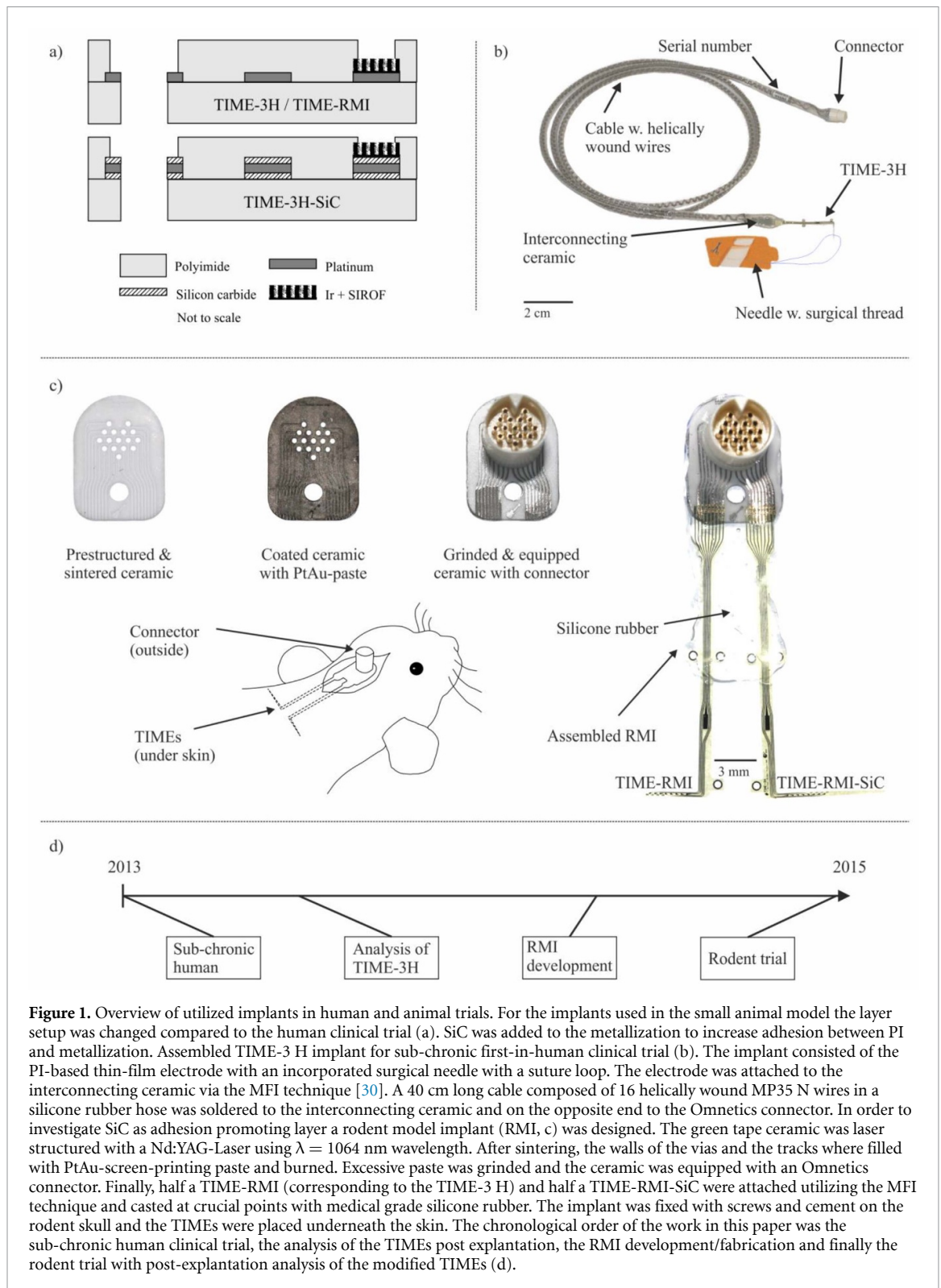
Figure 1. Overview of utilized implants in human and animal trials. For the implants used in the small animal model the layer setup was changed compared to the human clinical trial (a). SiC was added to the metallization to increase adhesion between PI and metallization. Assembled TIME-3 H implant for sub-chronic first-in-human clinical trial (b). The implant consisted of the PI-based thin-film electrode with an incorporated surgical needle with a suture loop. The electrode was attached to the interconnecting ceramic via the MFI technique [30]. A 40 cm long cable composed of 16 helically wound MP35 N wires in a silicone rubber hose was soldered to the interconnecting ceramic and on the opposite end to the Omnetics connector. In order to investigate SiC as adhesion promoting layer a rodent model implant (RMI, c) was designed. The green tape ceramic was laser structured with a Nd:YAG-Laser using $\lambda = 1064$ nm wavelength. After sintering, the walls of the vias and the tracks where filled with PtAu-screen-printing paste and burned. Excessive paste was grinded and the ceramic was equipped with an Omnetics connector. Finally, half a TIME-RMI (corresponding to the TIME-3 H) and half a TIME-RMI-SiC were attached utilizing the MFI technique and casted at crucial points with medical grade silicone rubber. The implant was fixed with screws and cement on the rodent skull and the TIMEs were placed underneath the skin. The chronological order of the work in this paper was the sub-chronic human clinical trial, the analysis of the TIMEs post explantation, the RMI development/fabrication and finally the rodent trial with post-explantation analysis of the modified TIMEs (d).

the surrounding tissue), values of LGND vs. stimulation sites or RGND vs. stimulation site are different in magnitude.

Despite electrodes with an impedance up to 250 kΩ can be driven by the stimulator with respect to its voltage swing, we included a technical safety margin in our considerations and defined $|Z| = 150$ kΩ as technical limit in our investigations.

The impedance measurements were performed intra-operatively to verify the correct positioning inside the nerve of the TIME by monitoring the voltage response [31, 32], and immediately after the surgical implant (day 0). Any electrode that would have been surgically disconnected or be 'hanging in air' instead of being in contact to tissue would result in a high impedance value and immediately indicate

necessary action. The measurement of the impedance, however, does not give any indication of proper placement within the nerve and does not allow any prediction of fiber excitation. The procedure was repeated on days 2, 11, 17 and 30 in order to track impedance changes during the course of the clinical trial, which give hints towards foreign body reactions and scarring around the electrodes and electrical electrode failure, in general.

2.1.5. Optical analysis of the explanted TIMEs from the human clinical trial.

The optical analysis of both, the stimulation and the ground contact sites was done after explantation using light microscopy (Leica DM400 M, Leica Microsystems GmbH, Wetzlar, Germany)—partially with polarization filters, to enhance visibility of surface irregularities and delamination. The view from the bottom side of the electrodes was of particular interest, as hereby delamination was better visible.

In order to analyze the properties of the layer setup, scanning electron microscopy (SEM) in combination with focused ion beam (FIB, Zeiss Auriga 60, Carl Zeiss AG, Oberkochen, Germany) was utilized to gather cross-sections of high resolution overviews of the contact sites and the thin-film metallization.

After explantation of the TIMEs from the human clinical trial, 40 of 64 stimulation contacts (including not electrically connected contacts) and 5 out of 8 ground contacts were available for optical analysis.

During the optical analysis we focused on the distinction between delaminated and non-delaminated platinum thin-film metallization.

2.2. Measures to improve thin-film adhesion

After termination of the first-in-human clinical trial, adhesion failures could be ovserved within the thin-film metallization of the TIMEs. In parallel research we observed that SiC builds up good adhesion properties to both polyimide and platinum [1, 25]. Adhesion promotion layers that have been well established in silicon micromachining like chromium or titanium, for example, have not been taken into consideration. They either do not comply with biocompatibility measures, do not form strong covalent bonds to the polyimide or both [24, 33]. In order to improve mechanical stability we inroduced SiC as adhesion promoting layer between the metallization and the polymer substrate. We intended to obtain only adhesion and do not intend to use the material as dielectric shielding of electrical fields as done in other approaches [34].

2.2.1. Incorporation of SiC as adhesion promoter

The thin-film version TIME-RMI-SiC used the same design, but with a different layer setup in order to investigate SiC as adhesion promoting layer (figure 1(a) bottom).

Table 1. Thickness and Young's modulus of the single layer materials. Relevant layer setups for TIME-RMI tracks were PI-Pt-PI and for the TIME-RMI-SiC PI-SiC-Pt-SiC-PI respectively.

Material	Thickness t in μm	Young's modulus in GPa
Polyimide	5	9.8
SiC	0.05	153 [36]
Platinum	0.3	140 [37]

For the TIME-RMI-SiC—in order to evaluate SiC as adhesion promoter—a 50 nm layer of SiC was deposited using plasma-enhanced chemical vapor deposition (PECVD, PC310 reactor, STS Surface Technology Systems plc, Newport, UK) before evaporation of a 300 nm layer of platinum (Leybold Univex 500, Leybold Vacuum GmbH, Cologne, Germany) (figure S2b). Afterwards, another adhesion layer of 50 nm SiC was deposited via PECVD on the platinum (figure S2b1). All other fabrication process steps were the same for both TIME versions. SiC is intended to serve as adhesion promoting layer to the bottom as well as the top layer of polyimide for interconnect lines, contact pads and electrodes. Iridium and iridium oxide coating of the electrode sites was performed on top of the SiC layer for simplicity reasons without structuring of the SiC. We have proven elsewhere [24] the porous structure of these layers and evaluated the influence in the electrochemical characterization of the electrodes below as well as in current-voltage transfer characteristics of charge injection capacities. We have estimated the change of the mechanical strength by SiC incorporation to the original layer setup by adding the flexural rigidities of the SiC layers of a sample with rectangular cross section (track width $w = 15$ μm) within the described layer setup (table 1) and equation (1) [35].

$$EI_y = \sum_{i=1}^{n} E_i I_{yi} = \sum_{i=1}^{n} E_i \frac{w_i t_i^3}{12} \qquad (1)$$

The iridium and iridium oxide on the electrode contact sites have been neglected since they contribute to both setups in the same manner. The flexural rigidity of the TIME RMI-SiC is with the given parameters compared to the TIME RMI with about 0.002% larger. It was not considered as major mechanical stabilization factor for the devices as such in the animal experiments for the validation of the adhesion layers.

2.2.2. Assembly of test samples for preclinical in vivo validation.

The influence of the SiC layer on thin-film electrodes stability was performed in vivo in an animal model with the focus on electrode stability under electrical stimulation. Mechanical handling was excluded

intentionally in the animal model since it differs significantly from the human implantation procedure [13, 14, 19, 38]. *In vivo* verification concerning function and validation regarding stability of the thin-film metallization without and with additional SiC adhesion layers under electrical stimulation load was performed. For this, a rodent model implant (RMI) was developed, which allowed to implant and deliver stimulation with a TIME-RMI and a TIME-RMI-SiC simultaneously in the same animal (figure 1(c)).

The assembling technique in the RMI had to be adapted with respect to the study design. A high temperature co-fired ceramic (HTCC) made of aluminum oxide (HTCC 44000, ESL Europe, Agment Ltd., Reading, UK) served as carrier substrate. Details of this process can be found in Fiedler *et al* [39]. After lamination of four layers of the not-sintered HTCC Al_2O_3 substrate, vias and tracks were laser structured with a Q-switched Nd:YAG-Laser ($\lambda = 1064$ nm, DPL*Genesis* Marker, cab Produkttechnik GmbH & Co. KG, Karlsruhe, Germany). Afterwards, the substrate was sintered according to the datasheet in a high temperature furnace for 2 h at 1500 °C. The walls of the vias and the complete tracks were filled with PtAu screen-printing paste (5837-G, ESL Europe, Agment Ltd., Reading, UK) and fired according to the datasheet in a furnace (PEO-601, ATV-Technologie GmbH, Vaterstetten, Germany). Excessive screen-printing paste was removed by grinding.

The design was chosen to fit a commercially available connector (NCS-DD-16, Omnetics Connector Corporation, Minneapolis, MN, USA). This connector was soldered from the backside of the substrate after removing the connector pins. Excessive solder was removed by grinding. The design of the tracks was customized according to the microflex interconnection technique (MFI) structure [30].

For validating both TIME-RMI and TIME-RMI-SiC, at the same time in the same animal, the thin-film electrodes were cut at the middle line, so it was possible to attach both thin-film versions next to each other (figure 1(c)). After bonding using the MFI technique, the thin-film electrodes were stabilized mechanically with epoxy (UHU Endfest Plus 300, Bolton Adhesives, Rotterdam, Netherlands). To prevent shorts and corrosion of metal parts, the unprotected parts of the implant were casted in medical grade silicone rubber (MED-1000, NuSil Technology LLS, Carpinteria, CA, USA) (figure 1(c)). In total we used four devices in four rats.

Electrochemical properties of the RMI have been characterized by electrochemical impedance spectroscopy before implantation and after explantation. Details are given in the supplementary material.

2.2.3. Animal trials in a rodent model.
Four RMI devices described above were built up, characterized and prepared for implantation in order to analyze the long-term stability under chronic stimulation conditions in a rodent model (figure 1(d)). All experimental procedures performed were approved by the Ethical Committee of the Universitat Autònoma de Barcelona in accordance with the European Communities Council Directive 2010/63/EU, and in compliance with the NIH Guide for Care and Use of Laboratory Animals. Surgical procedures were performed in four Sprague-Dawley rats under pentobarbital anesthesia (40 mg kg^{-1} i.p.). The devices were mounted on the skull and fixed with three screws and dental cement. The thin-film part was carefully located underneath the skin of the dorsum of the rat (figure 1(c)). The subcutaneous location was preferred to an intraneural implant for two main reasons: it allowed to have one TIME-RMI and one TIME-RMI-SiC implanted under exactly the same environment conditions, and it did not induce discomfort to the animal over hours of continuous stimulation. The focus of this study was not on the mechanical impact on the complete device during handling and surgical intervention but on changes of intrinsic thin-film metallization stress generated by physiological environments and the changes associated to foreign body reaction under electrical stimulation. The wound was closed around the connector, allowing the experimenter connecting the devices to an external stimulator setup (STIM'nD, INRIA, Montpellier, France & Axonic, Vallauris, France).

The RMIs were used to deliver stimulation through both TIME-RMI and TIME-RMI-SiC arms contact sites. Two stimulation sessions of 90 min per day were performed. Rectangular, charge-balanced stimulation pulses were applied with an intensity of $I = 140$ μA, a pulse-width of $p_w = 150$ μs and a frequency of $f = 50$ Hz. Due to time and equipment limitations only 5 contacts (both GNDs, two SiC containing contact sites and one contact site w/o SiC; always the same site for comparison reasons like identical voltage drop) were stimulated on every RMI/animal. The RMIs were maintained implanted up to 1 month. A median stimulation period of 78 h per animal (representing 14 million pulses) was performed, which corresponds to about more than two months of stimulation with the clinical protocol of the previous human study [22] as well as of envisioned chronic human clinical trials in future.

2.2.4. Optical analysis of explanted thin-film electrodes from animal trials.
For the RMI thin-films the same optical analysis methods as described above were applied. In detail, 24 stimulation contacts and 4 ground contacts were available for TIME-RMI electrodes and 24 stimulation contacts and 3 ground contacts in case of the TIME-RMI-SiC.

2.3. Statistical analysis
The data acquired *in vivo* was longitudinal and unbalanced for each time point (days). Moreover, the data
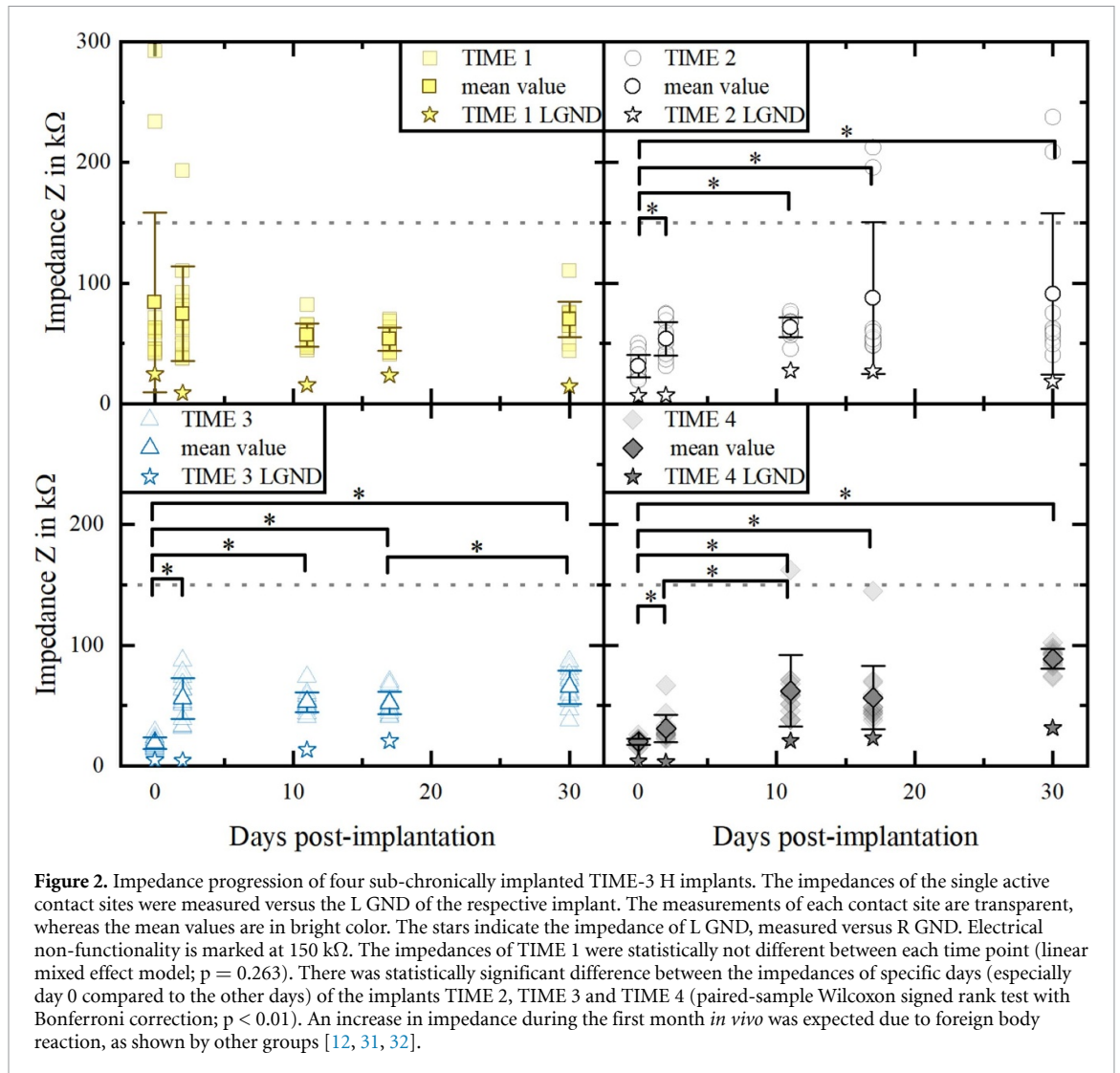
Figure 2. Impedance progression of four sub-chronically implanted TIME-3 H implants. The impedances of the single active contact sites were measured versus the L GND of the respective implant. The measurements of each contact site are transparent, whereas the mean values are in bright color. The stars indicate the impedance of L GND, measured versus R GND. Electrical non-functionality is marked at 150 kΩ. The impedances of TIME 1 were statistically not different between each time point (linear mixed effect model; p = 0.263). There was statistically significant difference between the impedances of specific days (especially day 0 compared to the other days) of the implants TIME 2, TIME 3 and TIME 4 (paired-sample Wilcoxon signed rank test with Bonferroni correction; p < 0.01). An increase in impedance during the first month *in vivo* was expected due to foreign body reaction, as shown by other groups [12, 31, 32].

was not normal distributed and the variance was not homogeneous. Therefore, we applied a linear mixed effect model for statistical analysis using the software R (version 3.5.2, The R Foundation for Statistical Computing, Vienna, Austria) and RStudio (version 1.1.463, RStudio Inc. Boston, MA, USA), which is robust to non-normality and unbalanced data sets. A paired-sample Wilcoxon signed rank test (OriginPro 2019, Version 9.6.0.172, OriginLab Corporation, Northampton, MA, USA) with a Bonferroni correction was applied in case of significant differences.

3. Results

3.1. Electrical characterization of the TIMEs *in vivo* (human)

The impedance of each single stimulation contact site and ground contact was recorded in the sub-chronic human clinical trial for all implants. The stimulation contacts were measured versus L GND (figure 2) and (R) GND (supplementary material). Depending on the implantation procedure, either L GND or R GND was facing the nerve's surface while the

other was on the opposite site towards the surrounding tissue. Since current pathways were different in both cases, the resulting voltage drop with the associated impedance magnitude was distinct too. The same procedure was performed for the GNDs. The impedance increased during the 30 d as expected due to the foreign body reaction (figure 2). TIME 1 exhibited on day 0 (just after implantation) large variability, with a median impedance of 84 kΩ ± 75 kΩ, that decreased during the course of the trial. The L GND contact exhibited a mean impedance of 17 kΩ ± 6 kΩ (figure 2, upper left). TIME 2 had increasing impedance from 31 kΩ to 91 kΩ together with increasing variation from 9 kΩ to 67 kΩ. On the last day, six contacts out of 14 had an impedance higher than 150 kΩ or even not measurable and were above our predefined threshold. The L GND contact showed stable impedance lower than 27 kΩ throughout the clinical trial (figure 2, upper right). The impedance of the contact sites of TIME 3 remained stable throughout the study, at around 60 kΩ, except at day 0, when the impedance was 19 kΩ. The impedance of the L GND was not measurable on day 30 (figure 2,

Table 2. Optically analyzed contact sites of explanted human TIME devices.

Cont. type	Total av.	Delaminated metallization	
		#	%
Stim. con.	40	25	62.5
GND	5	5	100

lower left). The impedances of the active sites on TIME 4 increased from 20 kΩ $\pm$ 3 kΩ on day 0 to 89 kΩ $\pm$ 8 kΩ on day 30. The impedance of the L GND in TIME 4 increased along the trial (figure 2, lower right) from 4 kΩ to 31 kΩ. In total, the mean impedance of all stimulation contact sites increased from 39 kΩ $\pm$ 46 kΩ to 78 kΩ $\pm$ 33 kΩ, measured against the L GND of the respective device. In total, 50 of the 56 stimulation contact sites (90 %) and seven of the eight GND sites (87.5%) were electrically working well on the last day before explantation. Every TIME had at least one electrically working GND at day 30 over which the stimulation sites could lead their current back to the stimulator.

No significant difference was observed in the impedance of TIME 1 at different days' post implantation ($p > 0.05$). For the other implants, there was a significant increase in the impedance over time ($p < 0.05$, paired-sample Wilcoxon signed rank test with a Bonferroni correction) (figure 2). TIME 4 was stable until day 17, but increased significantly ($p < 0.01$) on the last day.

Data recorded with R GND was similar to that of L GND and can be found in the supplementary material.

3.2. Optical analysis of explanted TIME implants (human)

Optical analysis of the explanted electrode contact sites focused on thin-film integrity revealed that 62.5% of the available stimulation contact sites and all the available ground contacts delaminated (table 2). This delamination of the thin-film metallization always appeared between the PI and the platinum interface as adhesion failure, never between platinum and SIROF. No cohesion failure of polyimide-polyimide not between iridium oxide and platinum was observed.

The R GND contact of the implant TIME 3 delaminated almost entirely (figure 3), in accordance to an electrical failure (figure 2). The metallization lifted from the PI. The

platinum showed a jagged breaking line. In contrast, TIME 1 GNDs were found partially/fully delaminated even though they have been electrically functional prior to explantation (figure 2). The contact site L6 on TIME 2 was electrically functional until the end of the clinical trial, and there was no sign of mechanical failure (figure 3), only some dried salt crystals. A more detailed cross-section view

indicated a crack formation in the SIROF, near the PI-substrate-metal transition (figure 3, black arrow). L8 on the implant TIME 2 was not electrically connected and consequently not stimulated during implantation, however, the delamination of the thin-film metallization was severe.

3.3. Optical analysis of explanted RMIs (rodent trial)

Comparing the stimulation contact sites, 87.5% of the TIME-RMI sites (without SiC adhesion promotion layers) were delaminated in contrast to 0% of the TIME-RMI-SiC (table 3). Three contacts of the TIME-RMI used for extensive stimulation were analyzed and two failed. In the TIME-RMI-SiC none of the 5 contacts used for stimulation failed. Concerning the ground contacts, all investigated

grounds without SiC as adhesion promoter exhibited delamination, even absence of the entire metallization (figure 4), whereas the ground contacts with SiC underneath the platinum all were intact (figure 4).

TIME-RMI thin-film electrodes delaminated in the RMIs, showing adhesion failure of the platinum-SIROF-sandwich and the PI, as well as crack formation with resulting delamination of the metallization (figure 4, RMI 3 and RMI 4). In contrast, the contact sites of the TIME-RMI-SiC preserved adhesion, despite slight crack formation, which did not lead to delamination over the implantation period (figure 4, RMI 1, TIME-RMI-SiC R1 arrow).

PI-based thin-film electrodes were analyzed from the bottom side using optical microscopy with polarization filters. SiC exhibited a blue appearance (figures 5(a) and (b)). Cracks were visible as whitish lines (figure 5(b), arrow). At the edge of the metallization, SiC exhibited a frizzy contour. As no interferences occurred, both contacts a and b in figure 5 did not delaminate. On the contrary, the contacts without SiC (shiny appearance) showed interferences indicative of delamination due to height changes. Crack formation could be observed along the overlapping PI edge together with delamination (figure 5(c), arrow). Also crack formation through the whole contact site causing delamination occurred (figure 5(d), arrow).

4. Discussion

We have evaluated the performance of TIME thin-film electrodes designed and developed for a first-in-human clinical trial with a duration of 30 d in accordance with European medical device regulations. These electrodes proved good functionality for electrical stimulation in about 90% of the stimulation contact sites which seemed to be in accordance with all the preclinical studies [14–19] that have been performed with respect to this implantation period. Since the ultimate goal is to apply such micro
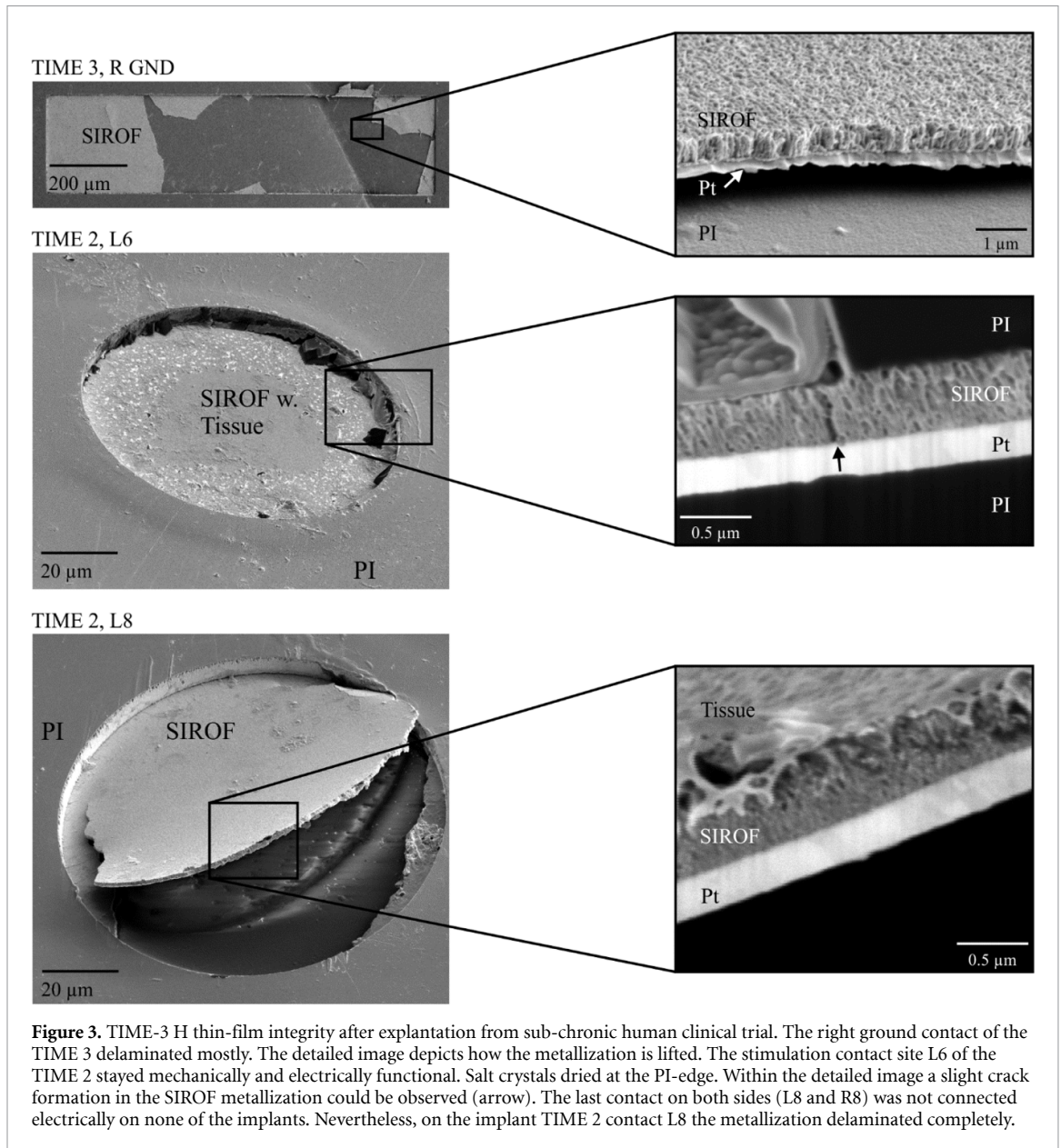
Figure 3. TIME-3 H thin-film integrity after explantation from sub-chronic human clinical trial. The right ground contact of the TIME 3 delaminated mostly. The detailed image depicts how the metallization is lifted. The stimulation contact site L6 of the TIME 2 stayed mechanically and electrically functional. Salt crystals dried at the PI-edge. Within the detailed image a slight crack formation in the SIROF metallization could be observed (arrow). The last contact on both sides (L8 and R8) was not connected electrically on none of the implants. Nevertheless, on the implant TIME 2 contact L8 the metallization delaminated completely.
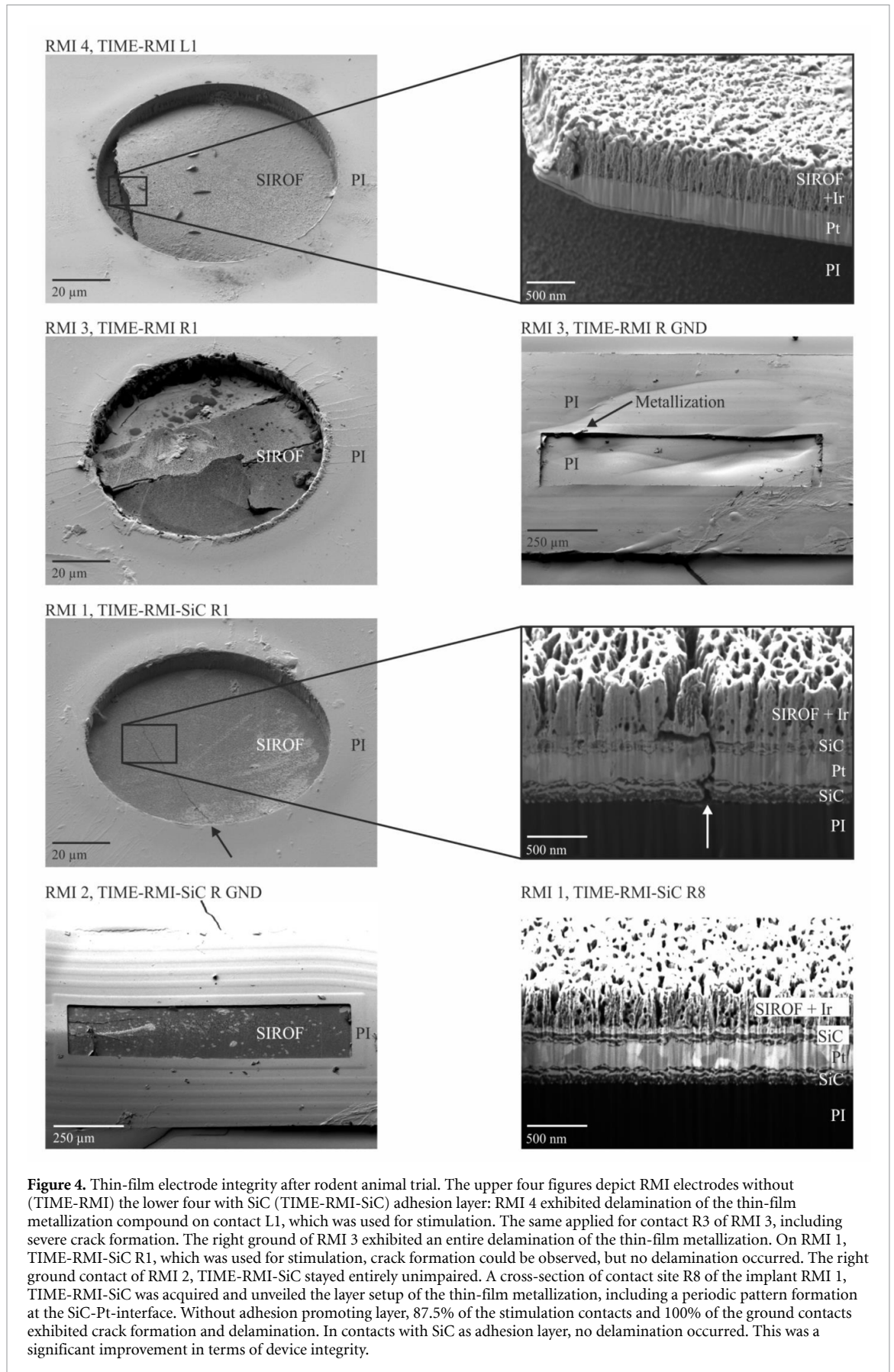
Table 3. Optically analyzed contact sites of explanted RMIs.

El. type	Cont. type	Total av.	Delaminated metallization		Used for stim	Delaminated metallization	
			#	%		#	%
TIME-RMI	Contact	24	21	87.5	3	2	66.6
TIME-RMI-SiC	Contact	24	0*	0	5	0*	0
TIME-RMI	GND	4	4	100	4	4	100
TIME-RMI-SiC	GND	3	0*	0	3	0*	0

implants for years, careful analysis of changes in the electrode metal and the metal-polymer compound were done in a post-explantation study by means of light and scanning electron microscopy in addition to impedance spectroscopy measurements. Results from electrical characterization at the last day before explantation were not in accordance with data from optical and electron microscopic investigations. The observations indicated that the adhesion between metals and polymer substrate and insulation layers

failed and needed to be improved for ensuring functionality and stability beyond 30 d.

This study here was designed with three objectives for evaluation of the used technology with respect to long-term stimulation applications and the technology transfer towards chronic clinical trials. We aimed to ascertain (1) the stability of the electrochemical transfer function of the stimulation sites over the implantation period and whether the stimulation thresholds stay within the chemical safe charge

Figure 4. Thin-film electrode integrity after rodent animal trial. The upper four figures depict RMI electrodes without (TIME-RMI) the lower four with SiC (TIME-RMI-SiC) adhesion layer: RMI 4 exhibited delamination of the thin-film metallization compound on contact L1, which was used for stimulation. The same applied for contact R3 of RMI 3, including severe crack formation. The right ground of RMI 3 exhibited an entire delamination of the thin-film metallization. On RMI 1, TIME-RMI-SiC R1, which was used for stimulation, crack formation could be observed, but no delamination occurred. The right ground contact of RMI 2, TIME-RMI-SiC stayed entirely unimpaired. A cross-section of contact site R8 of the implant RMI 1, TIME-RMI-SiC was acquired and unveiled the layer setup of the thin-film metallization, including a periodic pattern formation at the SiC-Pt-interface. Without adhesion promoting layer, 87.5% of the stimulation contacts and 100% of the ground contacts exhibited crack formation and delamination. In contacts with SiC as adhesion layer, no delamination occurred. This was a significant improvement in terms of device integrity.

injection limit, (2) which lessons can be learned from explanted devices regarding the material interfaces as well as the surgical handling during explantation and (3) if one can estimate device longevity and reliability based on electrical *in vivo* data obtained during stimulation.
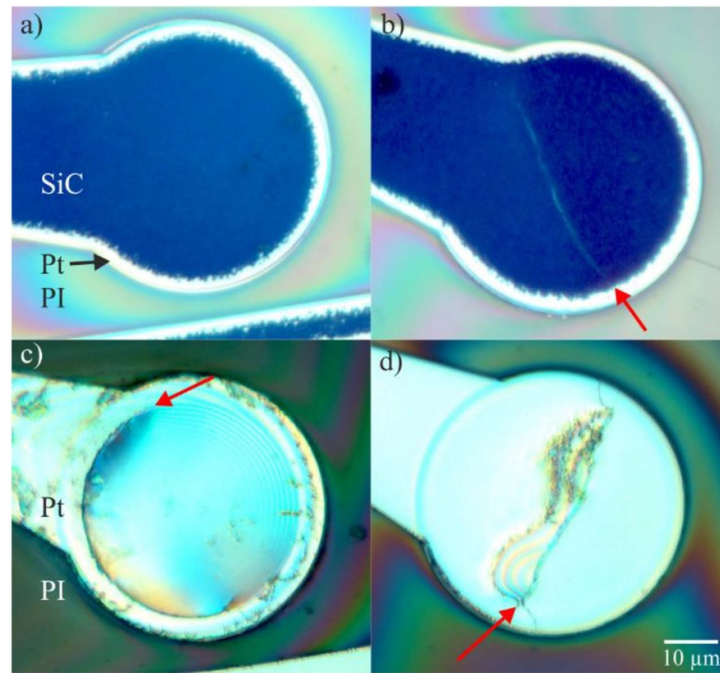
Figure 5. Microscopic view on the electrode backside through the bottom layer polyimide. A polarization filter was used to make delamination visible. SiC of the TIME-RMI-SiC thin-film displayed a blue appearance (a and b). Crack formation could be observed as a whitish line through the metallization (arrow in b). The TIME-RMI without SiC as adhesion promoting layer displayed a shiny appearance (c and d). Delamination was made visible with polarization filters, displaying interferences (c). Crack formation alongside the PI-overlap could be observed (arrow in c). Moreover, crack formation through the contact with partial delamination occurred (arrow in d) without SiC adhesion layer.

4.1. Electrical characterization of the TIME implants *in vivo* during the human clinical trial

Electrode impedance characterization via voltage transient magnitude over electrical current pulse magnitude ratio *in vivo* with one stimulation site versus one ground is a viable measure to evaluate the electrical functionality over the implantation time [31, 32] and to estimate the access resistance that originates from the tissue between the electrodes under test. It is a rough indirect estimate of the influence of foreign body reaction and fibrotic tissue encapsulation. In the human trial, 50 out of 56 stimulation contacts (89.3%) and 7 out of 8 ground contact sites (87.5%) were electrically functional after 30 d. On average, electrode impedance increased over the implantation period. Similar impedance increase over time was also found in other studies [12] and was correlated with the developing fibrosis around the implant [31]. Stimulation threshold increased but remained well below the maximum safe charge injection limit (determined to 120 nC) of the iridium oxide coating of the stimulation contacts sites that is higher than for platinum, which limited the use of electrodes in a previous study [12]. Since the perceptions of the subject remained stable over time [22], we believe that the foreign body reaction around the TIMEs fixated the electrodes well inside the nerve in addition to the surgical fixation on the epineurium and prevented movements during the implantation time.

4.2. Optical analysis of the TIME electrodes from the human clinical trial post-explantation

The explantation procedure at the end of the human study was performed prioritizing to minimize the time of the intervention and the potential damage to the subject nerve. The surgeon laid priority on the well-being of human subject exclusively and the protection of the nerve rather than on the integrity of the TIME devices to be explanted. Cables as well as the ceramic interconnector were tightly encapsulated by fibrous tissue, so a laborious dissection procedure was necessary to free cables and interconnects from this tissue to get explanted.

Therefore, several cuts were made to explant the TIMEs in pieces. *Ex vivo* evaluation of the TIME could not be made on complete devices but on fragments only. Therefore, electrochemical investigations were impossible to perform on the fragments. Especially the thin-film part of the TIME with the stimulation and the ground contact sites experienced mechanical forces during the explantation, that might have contributed to the delamination of the contact sites that had been already initiated during the implantation time due to decrease or loss of adhesion but did not deteriorate enough to lose electrical functionality. Moreover, even surgical high precision tools are by far larger than the stimulation contact sites and other sophisticated parts of the TIME implant, which makes it demanding to grab the thin-films at delicate structures while explantation without harming

their integrity. The thin-film part was designed for implantation solely and no particular handling flaps were designed for extraction.

Adhesion seemed to be at limit with the 30 d implantation period in the human trial with the chosen layer setup that had been validated in previous chronic animal experiments [19, 21] before being transferred to the clinical setting. The milieu of the foreign body reaction with reactive oxygen species, pH value shifts and other factors released might contribute to material changes by incorporation of oxygen and hydrogen species into the platinum thin-film layer and the iridium oxide coating. This could lead to increased stress that was above the value of the adhesion force of the platinum-polyimide sandwich.

Another possibility for mechanical failure could be caused by contacts of filopodia of macrophages in the fibrotic tissue due to the foreign body response [40] and the rough iridium oxide surface of the electrode structure, that might be stronger than the adhesion between the platinum and the underlying PI. Cells react on nanostructures on the surface [41] since they offer discrete attachment points. The topology of the nanostructures has a prevalent effect [42] and adhesion can be either increased (structures below 13 nm) or reduced (structures about 95 nm) [41]. Most investigations have been performed *in vitro* [42], with polymer surfaces [43] or materials close to bone implants like titanium and aluminum oxide. Oxygen rich surfaces as well as large roughness tend to lead to larger fibroblast attachment [43], but depending on the material, the larger initial cell attachment [41, 44] can eventually decrease fibroblast proliferation rate [45] on gold [46] and platinum [47]. Detailed analysis would be needed to solve the question of tissue adhesion on the electrode contact sites and the surrounding PI with samples that include part of the surrounding nerve and the implant as a compound sample. This topic goes far beyond the possibilities of this study since the major goal during the explantation procedure was to avoid damage to the remaining nerves of the patient.

As conclusion, adhesion forces of the PI-platinum compound have shown not to be sufficient for chronic implantation times and the benefit of adhesion layers to overcome this shortcoming had to be verified. The iridium oxide adhered well to the underlying platinum and did not cause any failure proving its applicability as coating for stimulation electrodes.

4.3. Outcome of preclinical study of TIME with improved metal-polymer adhesion

Integration of silicon carbide (SiC) was hypothesized by our group earlier as a potential solution to increase adhesion forces between platinum thin-film metallization and PI [1, 25]. TIME implants with a layer structure as used in the sub-chronic human implant study were compared to implants with additional SiC adhesion promotion layers underneath and

above the platinum towards the PI in a rat model. We purposely designed a TIME-RMI for subcutaneous implant on the dorsum in order to allow that the two arms of TIME-RMI and TIME-RMI-SiC remained under the same conditions and could be used for the same extensive electrical stimulation. Despite the TIME is designed for implantation within the peripheral nerve, we preferred this subcutaneous implant for avoiding other tethering forces and leads breaks that are frequent in electrode implants in the rat limbs [31, 40]. Nevertheless, the functional assessment of TIME chronic intraneural implant has been recently reported elsewhere [40].

Daily electrical stimulation for an accumulated average of 78 h over around 1 month implant time corresponded to the number of stimulation pulses estimated for the intermittent stimulation within the human clinical trial of about two months [22]. Since both TIME versions without and with SiC as adhesion promoting layers were implanted side by side, they experienced identical environmental conditions in the same animal (four animals in total), thus ensuring comparability of results. While implants without SiC adhesion layers showed adhesion loss and delamination in 87.5% of stimulation sites and 100% of ground contacts, none (0%) of the platinum metallization of the stimulation sites and ground contacts with additional SiC coating showed signs of adhesion loss and delamination. While adhesion between platinum and PI alone is caused on physisorption with low binding energy and interlocking effects [1, 24], SiC generates stronger covalent bonds to both, PI and platinum. The generation of platinum silicides mediates the chemisorption towards the platinum while direct bonds of the carbon atoms mediate adhesion to the carbon backbone of the PI. Intrinsic stress developed in both layer setups. However, low adhesion force without any adhesion layer was directly transferred in these cases to delamination while layer setups with SiC as adhesion layers showed no adhesion failure. In the worst case, in which intrinsic stress in the metal layer built up, the adhesion forces between SiC, platinum and polyimide were large enough to hold the compound together but stress release through crack formation occurred. Changes in electrode design based on simulations, e.g. reduction of site sizes and parallel arrangements to maintain overall geometrical site area are ways to further optimize stress distribution and thereby improve thin-film longevity.

5. Conclusion

Electrical functionality of the stimulation sites and the clinical outcome of a sub-chronic first-in-human study with TIME implants was excellent [22, 23] but analysis of the explanted TIMEs revealed that the PI substrate and the platinum thin-film metallization underneath the iridium oxide coating did not strongly adhere to each other, no matter whether the

electrode sites experienced electrical stimulation or not. More electrodes experienced adhesion loss than estimations from electrical functionality tests have been predicted. Adhesion needed to be improved for potentially higher patient safety and longer implantation periods. Silicon carbide (SiC) as adhesion promoter was introduced and established covalent bonds between SiC and platinum and PI, respectively, ensuring compound integrity and functionality even under intrinsic stresses during an *in vivo* study in a rat model with high stimulation regime. We believe that inclusion of such an adhesion layer and further pending measures reducing intrinsic stress (e.g. design changes) will increase device stability of the thin-film part to the level that these devices can be transferred into chronic clinical trials beyond the sub-chronic period of 30 d.

Acknowledgments

ORCID iDs

Paul Čvančara ⦿ https://orcid.org/0000-0003-2189-4413
David Guiraud ⦿ https://orcid.org/0000-0002-4184-6243
Thomas Stieglitz ⦿ https://orcid.org/0000-0002-7349-4254

References

[1] Ordonez J S, Schuettler M, Boehler C, Boretius T and Stieglitz T 2012 Thin films and microelectrode arrays for neuroprosthetics *MRS Bull.* **37** 590–8
[2] Navarro X, Krueger T B, Lago N, Micera S, Stieglitz T and Dario P 2005 A critical review of interfaces with the peripheral nervous system for the control of neuroprostheses and hybrid bionic systems *J. Peripher. Nerv. Syst.* **10** 229–58
[3] Rubehn B, Bosman C, Oostenveld R, Fries P and Stieglitz T 2009 A MEMS-based flexible multichannel ECoG-electrode array *J. Neural. Eng.* **6** 036003
[4] Schiefer M A, Tan D W, Sidek S M and Tyler D J 2016 Sensory feedback by peripheral nerve stimulation improves task performance in individuals with upper limb loss using a myoelectric prosthesis *J. Neural. Eng.* **13** 016001
[5] Charkhkar H, Shell C E, Marasco P D, Pinault G J, Tyler D J and Triolo R J 2018 High-density peripheral nerve cuffs restore natural sensation to individuals with lower-limb amputations *J. Neural. Eng.* **15** 056002

[6] Normann R A and Fernandez E 2016 Clinical applications of penetrating neural interfaces and Utah Electrode Array technologies *J. Neural. Eng.* **13** 061003
[7] Davis T S, Wark H A C, Hutchinson D T, Warren D J, O'Neill K, Scheinblum T, Clark G A, Normann R A and Greger B 2016 Restoring motor control and sensory feedback in people with upper extremity amputations using arrays of 96 microelectrodes implanted in the median and ulnar nerves *J. Neural. Eng.* **13** 036001
[8] Hassler C, Boretius T and Stieglitz T 2011 Polymers for neural implants *J. Polym. Sci.* B **49** 18–33
[9] Cogan S F 2008 Neural stimulation and recording electrodes *Annu. Rev. Biomed. Eng.* **10** 275–309
[10] Stieglitz T, Beutel H, Schuettler M and Meyer J-U 2000 Micromachined, polyimide-based devices for flexible neural interfaces *Biomed. Microdevices* **2** 283–94
[11] Rubehn B and Stieglitz T 2010 In vitro evaluation of the long-term stability of polyimide as a material for neural implants *Biomaterials* **31** 3449–58
[12] Rossini P M *et al* 2010 Double nerve intraneural interface implant on a human amputee for robotic hand control *Clin. Neurophysiol.* **121** 777–83
[13] Boretius T, Badia J, Pascual-Font A, Schuettler M, Navarro X, Yoshida K and Stieglitz T 2010 A transverse intrafascicular multichannel electrode (TIME) to interface with the peripheral nerve *Biosens. Bioelectron.* **26** 62–69
[14] Badia J, Boretius T, Andreu D, Azevedo-Coste C, Stieglitz T and Navarro X 2011 Comparative analysis of transverse intrafascicular multichannel, longitudinal intrafascicular and multipolar cuff electrodes for the selective stimulation of nerve fascicles *J. Neural. Eng.* **8** 036023
[15] Jensen W ed 2019 *Direct Nerve Stimulation for Induction of Sensation and Treatment of Phantom Limb Pain* (Gistrup: River Publishers)
[16] Boretius T 2013 *TIME: A Transverse Intrafascicular Multichannel Electrode (Biomedical Microtechnologies)* vol 4 (Uelvesbüll: Der Andere Verlag)
[17] Boretius T, Yoshida K, Badia J, Harreby K, Kundu A, Navarro X, Jensen W and Stieglitz T 2012 A transverse intrafascicular multichannel electrode (TIME) to treat phantom limb pain — towards human clinical trials *Proc. of the IEEE Int. Conf. on Biomedical Robotics and Biomechatronics* pp 282–7
[18] Stieglitz T, Schuettler M, Rubehn B, Boretius T, Badia J and Navarro X 2011 Evaluation of polyimide as substrate material for electrodes to interface the peripheral nervous system *2011: 5th Int. IEEE/EMBS Conf. on Neural Engineering* pp 529–33
[19] Badia J, Boretius T, Pascual-Font A, Udina E, Stieglitz T and Navarro X 2011 Biocompatibility of chronically implanted transverse intrafascicular multichannel electrode (TIME) in the rat sciatic nerve *IEEE Trans. Biomed. Eng.* **58** 2324–32
[20] Kundu A, Harreby K R, Yoshida K, Boretius T, Stieglitz T and Jensen W 2014 Stimulation selectivity of the 'thin-film longitudinal intrafascicular electrode' (tfLIFE) and the 'transverse intrafascicular multi-channel electrode' (TIME) in the large nerve animal model *IEEE Trans. Neural Syst. Rehabil. Eng.* **22** 400–10
[21] Harreby K R, Kundu A, Yoshida K, Boretius T, Stieglitz T and Jensen W 2015 Subchronic stimulation performance of transverse intrafascicular multichannel electrodes in the median nerve of the Göttingen minipig *Artif. Organs* **39** E36-E48
[22] Raspopovic S *et al* 2014 Restoring natural sensory feedback in real-time bidirectional hand prostheses *Sci. Transl. Med.* **6** 222ra19
[23] Oddo C M *et al* 2016 Intraneural stimulation elicits discrimination of textural features by artificial fingertip in intact and amputee humans *Elife* **5** e09148
[24] Ordonez J S 2013 *Miniaturization of Neuroprosthetic Devices and the Fabrication of a 232-channel Vision Prosthesis with a Hermetic Package (Biomedical Microtechnologies)* vol 5 (Uelvesbüll: Der Andere Verlag)

[25] Ordonez J S, Boehler C, Schuettler M and Stieglitz T 2012 Improved polyimide thin-film electrodes for neural implants *Conf. Proc. IEEE Eng. Med. Biol. Soc.* **2012** 5134–7

[26] Barrese J C, Rao N, Paroo K, Triebwasser C, Vargas-Irwin C, Franquemont L and Donoghue J P 2013 Failure mode analysis of silicon-based intracortical microelectrode arrays in non-human primates *J. Neural. Eng.* **10** 066014

[27] Barrese J C, Aceros J and Donoghue J P 2016 Scanning electron microscopy of chronically implanted intracortical microelectrode arrays in non-human primates *J. Neural. Eng.* **13** 026003

[28] Daschner R, Greppmaier U, Kokelmann M, Rudorf S, Rudorf R, Schleehauf S and Wrobel W G 2017 Laboratory and clinical reliability of conformally coated subretinal implants *Biomed. Microdevices* **19** 7

[29] George J A, Page D M, Davis T S, Duncan C C, Hutchinson D T, Rieth L W and Clark G A 2020 Long-term performance of Utah slanted electrode arrays and intramuscular electromyographic leads implanted chronically in human arm nerves and muscles (submitted) (https://doi.org/10.1101/2020.03.30.016683)

[30] Stieglitz T, Beutel H and Meyer J-U 2000 'Microflex'—A new assembling technique for interconnects *J. Intell. Mater. Syst. Struct.* **11** 417–25

[31] Wurth S *et al* 2017 Long-term usability and bio-integration of polyimide-based intra-neural stimulating electrodes *Biomaterials* **122** 114–29

[32] Williams J C, Hippensteel J A, Dilgen J, Shain W and Kipke D R 2007 Complex impedance spectroscopy for monitoring tissue responses to inserted neural implants *J. Neural. Eng.* **4** 410–23

[33] Stensaas S S and Stensaas L J 1978 Histopathological evaluation of materials implanted in the cerebral cortex *Acta Neuropathol.* **41** 145–55

[34] Cogan S F, Edell D J, Guzelian A A, Ping Liu Y and Edell R 2003 Plasma-enhanced chemical vapor deposited silicon carbide as an implantable dielectric coating *J. Biomed. Mater. Res.* A **67** 856–67

[35] Hassler C, Guy J, Nietzschmann M, Plachta D T T, Staiger J F and Stieglitz T 2016 Intracortical polyimide electrodes with a bioresorbable coating *Biomed. Microdevices* **18** 81

[36] El Khakani M A, Chaker M, Jean A, Boily S, Kieffer J C, O'Hern M E, Ravet M F and Rousseaux F 1994 Hardness and Young's modulus of amorphous a -SiC thin films determined by nanoindentation and bulge tests *J. Mater. Res.* **9** 96–103

[37] Salvadori M C, Brown I G, Vaz A R, Melo L L and Cattani M 2003 Measurementnanostructured platinum surfaces of the elastic modulus of nanostructured gold and platinum thin films *Phys. Rev.* B **67** 153404

[38] Krähenbühl S M, Čvančara P, Stieglitz T, Bonvin R, Michetti M, Flahaut M, Durand S, Deghayli L, Applegate L A and Raffoul W 2017 Return of the cadaver: key role of anatomic dissection for plastic surgery resident training *Medicine* **96** e7528

[39] Fiedler E, Ordonez J S, Stieglitz T, Fiedler E, Ordonez J S and Stieglitz T 2013 Laser-structured ceramic adapters for reliable assembly of flexible thin-film electrodes *Biomed. Tech.* **58**

[40] de la Oliva N, Navarro X and Del Valle J 2018 Time course study of long-term biocompatibility and foreign body reaction to intraneural polyimide-based implants *J. Biomed. Mater. Res.* A **106** 746–57

[41] Anselme K, Davidson P, Popa A M, Giazzon M, Liley M and Ploux L 2010 The interaction of cells and bacteria with surfaces structured at the nanometre scale *Acta Biomater.* **6** 3824–46

[42] Variola F *et al* 2009 Improving biocompatibility of implantable metals by nanoscale modification of surfaces: an overview of strategies, fabrication methods, and challenges *Small* **5** 996–1006

[43] Patrito N, McCague C, Norton P R and Petersen N O 2007 Spatially controlled cell adhesion via micropatterned surface modification of poly(dimethylsiloxane) *Langmuir* **23** 715–9

[44] Ni S, Sun L, Ercan B, Liu L, Ziemer K and Webster T J 2014 A mechanism for the enhanced attachment and proliferation of fibroblasts on anodized 316L stainless steel with nano-pit arrays *J. Biomed. Mater. Res. Part* B **102** 1297–303

[45] Elter P, Weihe T, Lange R, Gimsa J and Beck U 2011 The influence of topographic microstructures on the initial adhesion of L929 fibroblasts studied by single-cell force spectroscopy *Eur. Biophys. J.* **40** 317–27

[46] Chapman C A R, Chen H, Stamou M, Biener J, Biener M M, Lein P J and Seker E 2015 Nanoporous gold as a neural interface coating: effects of topography, surface chemistry, and feature size *ACS Appl. Mater. Interfaces* **7** 7093–100

[47] Pennisi C P, Sevcencu C, Dolatshahi-Pirouz A, Foss M, Hansen J L, Larsen A N, Zachar V, Besenbacher F and Yoshida K 2009 Responses of fibroblasts and glial cells to nanostructured platinum surfaces *Nanotechnology* **20** 385103